Title
ATOMIC AND MOLECULAR PROCESSES AT SOLID SURFACES

Author
Somorjai, G.A.

Publication Date
1976-07-01

Submitted to Journal of Colloid and Interface Science

LBL-5142
Preprint

ATOMIC AND MOLECULAR PROCESSES AT SOLID SURFACES

G. A. Somorjai

July 21, 1976

Prepared for the U. S. Energy Research and Development Administration under Contract W-7405-ENG-48

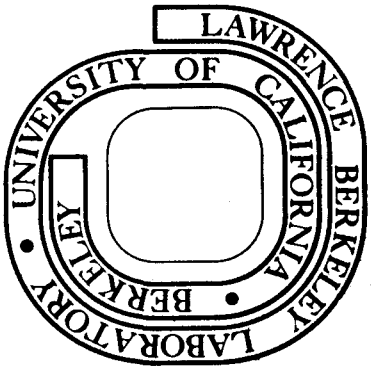

DISCLAIMER

LBL 5142

ATOMIC AND MOLECULAR PROCESSES AT SOLID SURFACES

by

G. A. Somorjai

Materials and Molecular Research Division, Lawrence Berkeley Laboratory,
and Department of Chemistry, University of California,
Berkeley, California 94720

Abstract

Developments of new techniques over the past 15 years permits the investigation of the structure, the composition and reactivity of solid surfaces on the atomic scale. Our present knowledge of the structure of clean surfaces and of adsorbed monolayers as studied by low-energy electron diffraction is reviewed. Surface crystallography provides information on the nature of the surface chemical bond.

Electron spectroscopy studies of the surface phase diagrams (surface composition vs. bulk composition and temperature) of binary alloy systems are reviewed. The surface enrichment of one of the alloy constituents is commonly observed. The various thermodynamic and chemical variables that control the surface composition are discussed.

The reactive scattering of molecular beams from surfaces reveals the kinetics and mechanisms of surface reactions. From the data the minimum

surface residence times of the reactants and products and the partitioning of energy between the molecules and the surface are determined. The available experimental data is reviewed and the utility of this technique is demonstrated by discussion of the H_2-D_2 exchange on platinum surfaces.

Introduction

In recent years a very large number of new techniques have become available that permit the investigation of surface phenomena on the atomic scale. Most of these involve the scattering of electrons, atoms, molecules or ions or photons (especially in the vacuum ultraviolet or higher energy range). Particles such as electrons and atoms are scattered very strongly by the topmost monolayer, thus the scattered species provide information primarily about the surface. Elastically scattered (diffracted) electrons in the 15-200 eV range are the probes utilized in low-energy electron diffraction to determine the structure of an ordered surface or of an adsorbate (surface crystallography). Electrons that are emitted from the valence shell or from the inner shells of surface atoms as a result of bombardment by electrons or photons of higher energy (10-10^4 eV) are the probes of ultraviolet photoelectron spectroscopy, Auger electro spectroscopy and X-ray photoelectron spectroscopy. These techniques are employed to determine the chemical composition of the surface and the oxidation states of surface atoms with a sensitivity of about 1% of a monolayer ($\sim 10^{13}$ atoms/cm^2). Once we know the arrangement and composition of atoms at the surface we may study a variety of surface phenomena involving atom transport such as surface reactions and establish how the reaction rate and reaction path leading to observed product distribution depends on the surface structure and composition. Reactive scattering of a beam of molecules that takes place upon their collision with the surface has been used to unravel the elementary surface reaction steps. Studies of surface reactions by molecular beam scattering reveal the minimum surface residence time of the reactant that leads to a chemical reaction, the reaction

probability (number of product molecules/number of incident reactant molecules) and the partitioning of energy (translation, vibration and rotation) among the reaction partners, the reactants, surface atoms and the desorbing product molecules. Other methods of studying chemical surface reactions at higher surface coverages than those used in molecular beam surface scattering experiments can also profit from relating the reactivity of the surface with its atomic structure and composition.

This paper will be divided into three parts. First we discuss our present knowledge of the atomic surface structure. Much of the atomic scale information has been obtained by low-energy electron diffraction studies over the past 15 years and these will be reviewed. Then we discuss what is known of the surface composition of multicomponent systems, primarily metal alloys since these have been studied in most detail. Finally, we shall review our present understanding of energy transfer during surface reactions and how the reactivity depends on the structure and composition of solid surfaces. We shall neglect discussions of the techniques that have been utilized. Reviews on the use of low-energy electron diffraction,[1,2,3] electron spectroscopy[4,5,6] and molecular beam scattering[7,8] are available and should be consulted by the interested reader.

The Structure of Solid Surfaces

Figure 1 depicts schematically a solid surface. The surface is structurally heterogeneous, there are several different atomic sites which are distinguishable by their number of nearest neighbors or coordination number. There are atoms in terraces where they are surrounded by the largest number of neighbors. There are atoms in steps, and at kinks in

the steps. These sites have less neighbors than the atoms in the terraces. Adatoms that are located on top of the terrace have, of course, the smallest coordination number. This model of the solid surface has been utilized to develop the theory of the growth of crystals and to explain the vaporization mechanisms of solids and other surface phenomena. New information that has been emerging from our studies, primarily single crystal surfaces, is that each of the surface sites may have different chemical reactivity.[9] Our studies of transition metal surfaces indicate that chemical bond breaking (H-H, C-H and C-C bonds) are facilitated at low coordination number sites such as atomic-steps and kinks that can be present on suitably prepared surfaces with high concentrations.[10,11]

If each crystal plane, step and kink sites at the surface have different chemical reactivity much of the complexity revealed in studies of heterogeneous catalysis or corrosion can readily be rationalized. Small particles used in heterogeneous catalysis for example are bound by different atomic planes and must have large concentrations of atoms in steps and in kink positions. A crystallographic model of one such particle is shown in Fig. 2. Thus the experimentally determined reaction rate and product distribution is that obtained by the sum total of the rates and products obtained at each surface site. It is very difficult, if not impossible, therefore, to decipher the reactivity of each active surface site from the experimental data. It is possible, however, to prepare surfaces of single crystals where one or another surface site is present

in large concentrations and study them by low-energy electron diffraction (LEED), a technique that can identify these various surface sites. A scheme of the LEED experiment is shown in Fig. 3a. Low-energy electrons (10-200 eV) are back-scattered from a crystal surface and the elastically scattered fraction (those electrons that did not lose energy in the collision with the surface) is accelerated and impinge on a fluorescent screen where the diffraction spots are displayed.[1] The diffraction patterns and schematic representations of the three types of surfaces of platinum that give large differences in relative concentrations of terrace, step and kink sites are shown in Fig. 3b. Surfaces where most of the atoms are in terrace

positions can be easily prepared and these exhibit high thermal and chemical stability. Alternately stable surfaces with over 20% of the surface atoms in step positions have been prepared. By appropriate cutting of a single crystal, one can introduce a high density of kinks into the steps.[11] One may explore the chemistry of each of these surface sites by studying the reactivity as a function of step or kink concentration on a series of single crystal surfaces and compare the results with those obtained on small particles. This is then the approach we took in many catalytic studies using single crystal platinum surfaces to explore the mechanism of hydrocarbon reactions.[11]

A. The Structure of Clean Solid Surfaces

There are perhaps two major findings that emerge from low-energy electron diffraction studies over the past 15 years that were previously not known.

1) Surface reconstruction. Many surfaces have atomic structures that are different from that expected from the projection of the X-ray bulk unit cell. The surface atoms assume new equilibrium positions by out of plane buckling or by "relaxing" inward (contraction) that often results in entirely different ordered surface structure.

2) Surfaces that exhibit ordered surface irregularities (steps and kinks) are the stable structure of crystal planes of high Miller index. A larger number of crystal planes are characterized by an atomic structure in which terraces of a few atoms wide are separated by periodic steps of one atom in height. This ordered step-terrace arrangement persists up to the melting point of many solids. We shall give examples of both of these properties of solid surface structure.

Figure 4 displays the diffraction patterns and schematic representation of the structures of the (100) crystal face of platinum. This surface exhibits the so-called (5x1) surface structure shown in the figure (Fig. 4a). There are two perpendicular domains of this structure and there are 1/5, 2/5 3/5 or 4/5 order spots between the (00) and (10) diffraction beams. The surface structure appears to be stable at all temperatures from 25°C to the melting point although at elevated temperatures impurities from the bulk can come to the surface and cause a transformation of this structure to the impurity stabilized (1x1) surface structure (Fig. 4c). Preliminary calculations by Clark et al.[12] and in this laboratory indicate that a model for Pt(100) in which the surface atoms assume a disordered hexagonal configuration by out-of-plane buckling is favored. The apparent (5x1) unit cell is then the result of the coincidence of the atomic position of atoms in the surface, i.e., in the distorted hexagonal layer, with atoms of the undistorted second layer below.

The surface atoms in any crystal face are in an anisotropic environment which is very different from that above the bulk atoms. The crystal symmetry that is experienced by each bulk atom is markedly higher than for atoms placed on the surface. The change of symmetry and the lack of neighbors in the direction perpendicular to the surface permit displacement of the surface atoms in ways that are not allowed the bulk. Surface relaxation can give rise to a multitude of surface structures depending on the electronic structure of a given substance. The (100) crystals of gold and iridium that are neighbors of platinum in the periodic table exhibit the same surface reconstruction and the same surface structure as that of platinum that is shown in Fig. 4. The (110) crystal faces of these

three elements are also restructured and exhibit a different unit cell than that expected from the bulk X-ray structure. The (111) crystal face of these three metals has the same surface structure as that indicated by the bulk unit cell. Other metals such as tin, antimony and bismuth also exhibit surface reconstruction. For semiconductors, however, most crystal planes that have been studied show reconstruction.[1,3] Monatomic (Si, Ge) and diatomic (GaAs, InSb, CdS, ZnO, etc.) semiconductor surfaces have been investigated in large numbers and surface reordering has been observed for most of them.[1,3] Frequently there are changes of surface structure with temperature (order-order transformation) that are often irreversible.

The mechanisms of surface reconstruction is not well understood. There are models invoking changes of electronic structure at the surface or proposing the presence of surface relaxation or ordered vacancies to explain these findings.[13] Further studies both experimental and theoretical are clearly necessary to understand the mechanism and nature of surface restructuring.

The excess free energy introduced by the creation of the surface induces other types of chemical changes as well in addition to surface reconstruction. Alkali-halide surfaces have unit cells not visibly different from what is expected from the bulk X-ray unit cells. However, the surface composition appears to be markedly different. Auger electron spectroscopy studies of alkali-halides revealed that excess vacancies are introduced,[13] the surface becomes enriched in either cations or in anions depending on the relative sizes of the positive ions. Oxide surfaces, such as the surface of aluminum oxide and vanadium pentoxide, exhibit both nonstoichiometry and change of surface structure.[14] It appears that under appropriate

conditions the cation is reduced at the surface and a lower oxidation state surface oxide forms (Al_2O or V_3O_5) with surface structure and composition that are different from that of the bulk oxide. Still another type of surface restructuring is exhibited by the surface of crystals of large organic molecules. For example, phthalocyanine crystals can be epitaxially grown on ordered metal surfaces.[15] When copper phthalocyanine was grown on the copper (111) surface the surface structure of the growing organic single crystal layer did not resemble the structure of any of the simpler crystal planes in the bulk structure of the organic crystal. It appears that the ordered metal substrate predetermined the orientation and packing of the phthalocyanine monolayer which in turn control the orientation and packing of organic layers deposited on top of it. For large molecules such as phthalocyanine restructuring into a more stable crystallographic arrangement requires molecular rotation and diffusion processes that are too slow to occur under conditions of crystal growth. Thus the molecules are frozen into a surface structure that is predetermined by the structure of the substrate and the first adsorbed organic monolayer.

The preparation of surfaces with large concentrations of stable and ordered irregularities (steps and kinks) can be carried out by cutting crystal surfaces along high Miller index directions. Figures 5a and 5b show the cutting angles to obtain surfaces with given step and kink densities and also shows the schematic representations of these surfaces. Stepped surfaces of several metals, semiconductors and oxide surfaces were prepared this way.[13] It appears that ordered steps of one atom in height separated by terraces of low Miller index orientation that are of many the same width, on the average, are the stable surface structures of high

Miller index surfaces of solids regardless of their chemical bonding. Not all stepped surfaces are stable however.[9] Figure 6 shows a stereographic triangle for platinum with all the crystal faces that were cut and studied in our laboratory indicated by the points on the triangle. With the exception of crystal faces in the regions indicated by arrows, the ordered step structure proved to be the stable surface structure on all these crystal faces. However, when a crystal face was cut that was located in the region indicated by one of the arrows (the (510) surface plane for example) this face was unstable and on heating it undergoes facetting into the two surfaces shown at the ends of the arrows (the (100) and (210) crystal faces). Thus studies of the relative structural stability of the various surfaces permits determination of their relative surface free energies (the more stable surfaces having the lower surface free energy).

In several studies of adsorption and surface reaction on platinum surfaces we have found that atomic steps and kinks are the active sites to break strong H-H, C-H and C-C chemical bonds. In the absence of high concentration of these sites (for example on the (111) surface) thermal activation or high adsorbate pressures were necessary to obtain bond breaking activity comparable to that detectable on stepped surfaces. Theoretical calculations by Falicov et al.[16,17,18] revealed two major reasons for this enhanced chemical activity of low coordination number surface sites. One of the reasons is that at a corner site there is enhanced amplitude of charge density fluctuations that leads to an increased potential energy ($\Delta\phi$) of free electrons on the corner atom. The magnitude of this potential energy difference for electrons at the corner site and away from it depends on the local atomic structure at the surface

irregularity. As a result, some of the free electrons are displaced away from the corner site leaving behind a net positive charge. The number of electrons ΔN that are removed from the corner site is proportional to $\Delta N \sim -\Delta\phi \times D(E_f)$ where $D(E_f)$ is the density of states at the Fermi level. The magnitude of $\Delta\phi$ is determined by the local step structure. Thus there is a large local electronic field present at the corner sites of the order of .3-.4 v/Å that should help to further polarize the incoming molecules that have well-defined polarizabilities and break them apart. The higher the density of states at the Fermi level, $D(E_f)$, the larger is the positive charge in the corner site. For transition metals the density of states at the Fermi level is very large indeed while for nontransition metals $D(E_f)$ can be quite small. Some of the values of $D(E_f)$ that have been determined are platinum: 2.1 e/v/atom; nickel: 1.1; tungsten: 0.7; copper: 0.4; and gold: 0.3. These values yield ΔN of -0.6, -0.3 and -0.2 for platinum, nickel and tungsten taking $\Delta\phi$ equal .3 volts. Thus, for metals with large values of $D(E_f)$ there are large variations of charge density at surface irregularities, i.e., low coordination number sites. For gold, on the other hand, ΔN is about -0.09. The surface irregularities for gold do not show much charge density variation with respect to atoms at surface sites away from steps. Therefore the gold surface is likely to present uniform charge density to the incoming reactants and is homogeneous regardless of variations of surface sites. These conclusions are certainly supported by our experiments of chemisorption and chemical reactions on platinum,[11] gold[19] and iridium[20,21] surfaces. While surface irregularities like atomic steps have different chemistry for platinum and iridium both metals with with high density of states, gold surfaces show the same chemical behavior

regardless of surface atomic structure.

The second reason for the different chemistry with changing coordination number is due to the local field experienced by the transition metal ion at various surface sites. This local field has two major effects: (1) causing a sizable electron transfer from the stepped corner to the bulk or vice versa; (2) producing different d-orbital level splittings and different d-orbital occupations depending on the position of the metal ion. Tsang and Falicov[17] have calculated the energy levels of localized d-electrons at different surface sites when the crystal field is turned on. These calculations made across the periodic table for ions with different number of d-electrons. The d-electron wave function is a product of the radial and the angular part. Assuming that the radial part is constant, they display the resultant constant contour of the angular part for these various ions. These contours clearly indicate that the stereochemistry of the corner atoms can be quite different from that of a terrace atom, therefore, a different kind of bonding is favored at different sites. The result of their calculations have been applied to explain the large differences between catalytic activity of various transition metal surfaces. Studies of the charge density, the energy and spatial arrangement of localized electronic orbitals at low coordination number surface sites, i.e., steps and kinks, appears to be an important and challenging area of theoretical surface chemistry.

B. The Structure of Adsorbed Monolayers

Over the past 15 years, low-energy electron diffraction studies of monolayers of adsorbates on crystal surface have shown that 1) adsorbate monolayers are largely ordered under proper conditions of the experiment,

2) the surface crystallography reveals the nature of the surface chemical bond and 3) there is a marked crystal plane sensitivity of the surface chemical bond. Surface irregularities and kinks have different bond breaking abilities as compared to atoms in terraces.

It is well established that atoms or small diatomic molecules order readily on low Miller index surfaces. There are over 200 surface structures that were detected have been tabulated.[1,22] In fact, the tabulated data permitted us to propose rules of ordering for these small molecules that allows prediction (within certain limits) of their surface structure.[23]

The surface structures over 50 hydrocarbon molecules have been studied on the platinum (111) and (100) surfaces. Again, ordering in the adsorbed monolayer was more of a rule than an exception. However, caution should be exercised in establishing the best experimental conditions to study ordering of the adsorbed layers. The same hydrocarbon molecule, benzene for example, that orders readily at 300 K on the Pt(111) surface may decompose readily on the Ir(111) surface or fail to adsorb altogether on the (111) surface of gold under identical experimental conditions. The metal-adsorbate interaction can be either too strong or too weak and thus ordering is prevented in the monolayer. Ordering can be facilitated by lowering the surface temperature since most bond breaking processes at the surface require activation energy or in case of weak surface bonding, lowered surface temperature results in increased surface coverage of the adsorbate.

Ordering of large molecules is generally best on high symmetry surfaces. (Pt(111) rather than Pt(100), for example). Aromatic molecules with high rotational symmetry order the best with small substituent groups

and at low incident vapor flux. These conditions allow maximum opportunity for a molecule, once adsorbed, to reorient itself for incorporation into the growing ordered region. Thus ordering of large molecules can be seen to be somewhat different from site adsorption for smaller molecules. In the former case the molecule may overlap many surface bonding sites and, beside requiring sufficient translational mobility, the molecule must also have sufficient rotational mobility.

The location of the adsorbed atom or molecule, its bond distances, bond angles with respect to other atoms in the surface can uniquely be determined by low-energy electron diffraction, from analysis of the diffraction beam intensities. Over the past 10 years the theory of low-energy electron diffraction has been developed to the point that we can determine the surface structure of simple adsorbates. The field of surface crystallography has been born.

In Table I we list the experimentally determined bond lengths that were obtained from surface crystallography studies of several adsorbed atoms on metal surfaces. These results are compared with the bond length obtained by summing the covalent radii. In most cases the differences are within .1 Å that is claimed for the uncertainty of the experimental determination, and in no case is the discrepancy greater than 10%. This result suggests that the chemisorption bond is basically covalent for these atoms which means that theoretical treatments in terms of localized surface complexes and clusters should be applicable to chemisorption. Recently we have analyzed the surface structure of the first adsorbed molecule, that of acetylene (C_2H_2), on the (111) crystal face of platinum.[25] The nature of bonding of this molecule to a metal surface has important

catalytic implications. Figure 7 shows the various molecular positions that were considered for C_2H_2 as possible bonding sites. It was concluded that acetylene is chemisorbed on platinum (111) in one of two possible local bonding modes at a distance of 1.95±.1 Å above the topmost plane of platinum atoms. In the most likely bonding mode (C_2) the molecule is centered on a triangular site, the carbon atoms are equivalent by symmetry and relevant C-Pt distances are 2.25 Å and 2.259 Å. In the other possible bonding mode (B_1) the molecule is in an approximately two-fold position with each carbon coordinating to three platinum atoms, the C-Pt distances being 2.47 Å and 2.65 Å. The C_2 mode of bonding is found to occur in various trimetallic metal-alkine complexes whereas the bridging structure analogous to B_1 occurs in bimetallic complexes. These findings and structure analysis contadicts popular notions of acetylene adsorption on transition metal surfaces that were thought to involve acetylene π-complex coordinated to a single metal atom (model geometry A_1 or A_2) or a di-sigma model has often been cited in connection with mechanism of dehydrogenation of ethylene, C_2H_4, to an acetylanic species upon adsorption with the ligand molecular orbitals in an sp^2 hybrid configuration. Although these bonding modes could be operable in some other bonding situations, they are not the favored bonding arrangements of acetylene on the Pt(111) surfaces.

Surface crystallography by low-energy electron diffraction permits us to determine the chemical bonding of atoms or simple molecules on solid surfaces. This information in turn will aid in determining the nature of the surface chemical bond. This may also aid our learning about adhesion and lubrication and other surface phenomena in the molecular level.

Surface irregularities, steps and kinks, play important roles in breaking chemical bonds that otherwise would not easily be broken in the absence of these sites. There are many reports of the variation of heats of adsorption and the types of binding states that are available, from crystal face to crystal face. A polycrystalline surface or the surfaces of small particles provide several bonding sites each with its own chemical activity. It is difficult to compare the reactivities of these structurally and therefore chemically heterogeneous surfaces that are prepared in different laboratories since minor changes in surface preparation changes their surface structure and thus may markedly alter their reactivity. It is therefore essential to correlate the atomic surface structure and reactivity of model systems such as single crystal surfaces and using the similarity in chemical reactivity between these crystal surfaces and polydispersed systems to learn about the atomic surface structure of dispersed small particles that are utilized frequently as heterogeneous catalyst systems.

The Surface Composition of Binary Alloys

The composition of alloys in the topmost monolayer is likely to be very different from the bulk composition for several reasons and we shall review briefly each one of them.

a) For systems that exhibit regular solution behavior, the surface free energy (which is always positive) is minimized by the segregation of that constituent with the lower surface tension. For metals that have high surface tensions as compared to organic surfaces or most oxide surfaces,

such surface enrichment is likely to be very marked indeed. For a system obeying regular solution theory, it has been shown[26,27] that the composition of the surface monolayer is given by Eq. (1).

$$\frac{x_1^A}{x_1^B} = \frac{x_b^A}{x_b^B} \exp\left(\frac{(\sigma^B - \sigma^A)a}{RT}\right) \exp\left[\frac{\Omega(\ell+m)}{RT}\left(\left(x_b^B\right)^2 - \left(x_b^A\right)^2\right) + \frac{\Omega\ell}{RT}\left(\left(x_1^A\right)^2 - \left(x_1^B\right)^2\right)\right] \quad (1)$$

Where x_1 and x_b are the atom fractions in the surface monolayer and bulk, respectively. In this expression σ is the surface energy, a is the molar surface area, T is the absolute temperature, R is the ideal gas constant, Ω is the regular solution parameter which is given from the heat of mixing ΔH_m by

$$\Omega = \Delta H_m / \left(x_b^B\, x_b^A\right) \quad (2)$$

The packing parameter ℓ gives the fraction of an atom's nearest neighbors which are in the same plane parallel to the surface as the atom. Similarly m is the fraction of nearest neighbors which are in an adjacent parallel plane. For instance, in an fcc lattice, an atom has 12 nearest neighbors so a (111) plane has 6 nearest neighbors in the plane of an atom and 3 nearest neighbors in the plane below the atom. Thus in this case ℓ = 6/12 and m = 3/12.

Electron spectroscopy techniques, especially Auger electron spectroscopy and photoelectron spectroscopy, have been eminently successful in determining the surface phase diagrams, i.e., the surface composition as a function of bulk composition and temperature, for several binary metal systems. A typical Auger spectrum of an alloy system that of silver--gold is shown in Fig. 8.[28] From the Auger peak intensities one may determine surface composition for a series of bulk compositions and from

this data the surface phase diagram is deduced. The most serious experimental difficulty in converting the Auger peak intensities to surface concentrations lies in estimating the depth near the surface from which the Auger electrons of different kinetic energy are emitted and the relative scattering power of the two types of atoms in this volume sampled by the electrons. Since part of the Auger signal is due to atoms below the surface, it is essential to subtract this part from the signal intensities in order to extract the surface contribution. Much of the discrepancy between results reported from different laboratories on the same alloy system can be attributed to difficulties in estimating relative contributions of surface atoms to the various Auger peak intensities.

b) Adsorbed gases or impurities segregating at the surface can markedly change the surface composition. If one of the constituents forms strong chemical bonds with the adsorbate (oxygen, CO, carbon, sulfur or calcium, most commonly) it will be accumulating on the surface even though that it may not be at the surface in the absence of the adsorbate. CO, for example, that forms strong bonds with many transition metal atoms may aid the segregation of these atoms at the surface at the expense of other constituents that form weak CO bonds. In essence an adsorbate converts a two-component system to a three component system thereby altering the surface composition at equilibrium.

c) Solute atoms with large or small radii with respect to the size of the solvent (majority) atoms may be "excluded" from the bulk because they introduce excessive strain in the crystal lattice. As a result, surface segregation of one component that is misfit in the crystal lattice can be observed. The strain energy contribution may enhance the surface

concentration of that component that would segregate on the surface on account of its effect of decreasing the total surface free energy. Conversely this strain energy contribution may oppose the effect of surface segregation of one constituent in some cases.

d) There are complex phase diagrams that exhibit the formation of stable compounds of high lattice energy. In this circumstance the energy necessary to exchange the two atoms, A and B, by removing them from their equilibrium lattice site is so large that it overrides the influence of surface forces that would induce surface segregation. Thus the bulk composition pins the surface composition, i.e., the surface and bulk compositions remain identical. We have found in studying the complex gold-tin phase diagram that this phenomenon occurs at the bulk composition of AuSn that forms a compound with high cohesive energy.

In Table II we list those metal systems that have been studied by electron spectroscopy and indicate which element is found in excess at the surface.

Since the topmost surface layer is the first line of defense of the solid against external chemical attack such as corrosion, it is essential that we determine and learn how to control the surface composition. Perhaps alloys with unique corrosion resistance under high temperature and high pressure conditions can be developed by the addition of small quantities of appropriately chosen constituents that passivate the surface layer by segregating there.

Molecular Beam-Surface Scattering

One of the important questions we must answer in order to unravel the

nature of surface reactions is how the energy partitions in a chemical reaction between the reactant, product molecules and the surface atoms.[7,8] Also it is useful to know the necessary minimum residence time of molecules on the surface for the chemical reaction to take place. To answer these questions we are studying the interaction of well-defined beams of molecules with crystal surfaces. The scheme of the molecular beam-surface scattering experiment is shown in Fig. 9. A beam of molecules impinges on the surface and the scattered product molecules are detected as a function of angle (angular distribution) by a rotatable mass spectrometer detector. By chopping the incident beams periodically the flight time of the molecules can be determined. This experimental information yields the surface residence time of the impinging molecules before readmission to the gas phase and the velocity and the momentum of the incident molecules and of the scattered products. The surface structure and composition of the crystal surfaces are also determined by simultaneously utilizing low-energy electron diffraction and Auger electron spectroscopy.

Using this sensitive molecular beam probe we have determined that the amount and type of energy transfer between the incident beam and surface depends very much on the surface structure and composition. Molecules scattered from ordered clean metal surfaces undergo little loss of their kinetic energy (velocity). If the surface is covered with a layer of adsorbed molecules, for example CO, the impinging atoms and molecules lose all their kinetic energy to the surface and are trapped long enough that complete energy equilibration occurs between the gas and the surface before the re-emission of the molecule.[29]

This effect is demonstrated in Fig. 10a and 10b. Here the linear signal intensity due to the scattered beam is plotted as a function of the scattering angle. The peaked angular distribution of hydrogen and the fact that the angle at which the scattered molecular beam has maximum intensity equals the angle of incidence of the incoming beam (which is indicated by the arrow at the abcissa) are characteristics of specular scattering (Fig. 10a). This type of ping-pong ball like scattering is associated with poor energy exchange between the incident gas molecules and the surface. In the case when the particles emitted from the surface have completely equilibrated with the surface, one obtains a cosine like angular distribution as shown in Fig. 10b. When hydrogen is scattered from a monolayer of adsorbed carbon monoxide, complete energy equilibration occurs between the incident molecules and the surface. Much of the energy accommodation between incident particles and the surface depends on the nature of energy transfer between the translational and rotational modes of the gas molecules (and vibrational modes if these can be excited or de-excited during the collision) and the vibrational modes of the surface atoms. It appears that the localized low frequency bending modes of adsorbed carbon monoxide are very effective in adsorbing much of the translational energy of the incident hydrogen molecules. A recent review summarizes the results of energy transfer studies during non-reactive molecular beam-surface scattering.[7]

Reactive scattering studies can be divided into two groups: 1) the reaction takes place on the surface under the catalytic influence of the surface atoms that however are not present among the reactants or the products (for example, $A_{2(gas)} + B_{2(gas)} \xrightarrow{\text{surface}} 2AB_{(gas)}$); 2) the surface atom is one of the reactants ($A_{2(gas)} + S \rightarrow SA_{2(gas)}$). Using a mass spectrometer

the product distribution and the rates of formation of the product molecules (reaction probabilities) are determined as a function of the system variables. From the dependence of the reaction rate on the incident beam velocity, the activation energy for adsorption (if any) is determined. From the surface temperature dependence of the rate, the activation energy of the surface reaction is obtained.

In Table III we list all of the pre-exponential factors, activation energies and reaction probabilities for the surface reactions that were studied by molecular beam scattering techniques and where such data were reported. From this information a great deal can be learned about the kinetics and mechanisms of surface reactions.

Let us consider, as an example, the mechanism of H-H bond breaking on platinum surfaces that can be investigated by studying the exchange of hydrogen and deuterium to form HD using molecular beam scattering.[30] One of the fundamental questions of heterogeneous catalysis is how surfaces lower the activation energy for simple reactions on the atomic scale so that they proceed readily on the surface while the same reaction in the gas phase is improbable. The reaction of hydrogen and deuterium molecules to form hydrogen deuteride is one of the simple reactions that takes place readily on metal surfaces, even at temperatures below 100 K. The same reaction is completely inhibited in the gas phase by the large dissociation energy of H_2 or D_2 (103 kcal/mole). Once the H_2 molecule is dissociated, the successive atom-molecule reaction ($H + D_2 = HD + D$) in the gas phase still has a potential energy barrier of about 10 kcal/mole. If we were to study this reaction at high pressures (about 10^3 Torr), the exchange takes place so rapidly on most transition metal surfaces that equilibrium

is readily established among the various hydrogen molecules, H_2, D_2 and HD. In order to study the kinetics of this reaction one has to carry out the experiments far from equilibrium. Molecular beam-surface scattering experiments work the best far from equilibrium at low incident beam pressures (about 10^{-7}-10^{-6} Torr) and at low surface coverages. The H_2-D_2 exhange reaction was studied by Bernasek et al.[30] using platinum single crystal surfaces of low and high Miller index. Under the conditions of the experiments which puts strict limitations on the residence time of the detected molecules the reaction product, HD, could not be detected from the (111) crystal face. However, the reaction product was readily detectable from the high Miller index stepped surface. The integrated reaction probability defined as total desorbed HD flux/H_2 flux incident on the surface is approximately 10^{-1} while HD formation was below the limit of detectability on the platinum (111) surface (reaction probability less than 10^{-5}). High Miller index single crystal surfaces are characterized by ordered arrangements of atomic steps of one atom height separated by terraces of low Miller index orientation. Thus atomic steps at the platinum surface must play controlling roles in dissociating the diatomic molecules. Fig. 11 shows the scattering distributions from both the (111) and the stepped platinum surfaces. Varying the chopping frequency of the incident molecular beams have yielded HD residence times of about 25 milliseconds and longer up to 1 second on a stepped platinum surface in the 700-1000 K surface temperature range. Such long residence times should result in complete thermal equilibration between the surface and the reactant products. Indeed it was found by experiments that the desorbing HD exhibits cosine angular distribution as seen in Fig. 11.

The reaction probability was also dependent on the angle of H_2 incidence. The maximum reaction probability was obtained upon incidence normal to the step edges. The experiments have also revealed that the exchange reaction occurs by a two-branch mechanism. The faster reaction takes place at the step while a slower reaction (with surface residence times of seconds) occurs on the atomic terraces. The absence of beam kinetic energy dependence of the rate indicates that adsorption and dissociation of hydrogen does not require activation energy. The surface is able to store a sufficiently large concentration of atoms which react with other surface atoms by a two-branch mechanism. The rate constants for the H_2-D_2 reaction were also determined under conditions of constant hydrogen atom coverage and are given in Table III. The rate determining step appears to be the diffusion of D atoms on the surface to a site where HD is formed by a two centered reaction subsequent to H_2 or D_2 dissociation at the step. At higher temperatures the reaction between an adsorbed H atom and an incident D_2 gas molecule may also become an important reaction channel. The catalyst action of the platinum surface for the exchange reaction is due to its ability to adsorb and dissociate hydrogen molecules with near zero activation energy and to store atomic hydrogen on the surface thereby converting the gas phase molecule-molecule reaction to an atom-atom reaction of low activation energy.

It would be of great importance to measure the velocity of the scattered products from time of flight measurements using a mass spectrometer, in addition to their angular distribution, in order to determine the nature of energy transfer between the HD product molecules and the surface prior to desorption. It is likely that during certain exothermic surface re-

actions (for example hydrogen or oxygen atom recombination) much of the chemical energy is converted into internal energy and translational energy of the product molecules. Studies of energy transfer during exothermic surface chemical reactions are in progress in several laboratories.

Acknowledgment

This work was supported by the U. S. Energy Research and Development Administration.

References

1. L. L. Kesmodel and G. A. Somorjai, MTP Int. Rev. Sci., Physical Chemistry Series 2, 7, 1 (1975).
2. J. B. Pendry, Low Energy Electron Diffraction. Academic Press, London, 1974.
3. J. A. Strozier, D. W. Jepsen and F. Jona in Surface Physics of Materials. J. M. Blakely, ed. Vol. 1. Academic Press, New York, 1975.
4. K. Siegbahn et al. ESCA-Atomic, Molecular and Solid State Structure Studied by Means of Electron Spectroscopy. Almqvist and Wiksells, Uppsala, 1967.
5. C. R. Brundle in Surface and Defect Properties of Solids. The Chem. Soc., 1, 171 (1972).
6. F. J. Szalkowski and G. A. Somorjai, Adv. High Temp. Chem., 4, 137 (1971).
7. S. L. Bernasek and G. A. Somorjai, Prog. in Surf. Sci., 5, 377 (1975).
8. S. B. Brumbach and G. A. Somorjai, Crit. Revs. in Solid State Sci., 4, 429 (1974).
9. G. A. Somorjai, Adv. in Catalysis, to be published 1976.
10. D. W. Blakely and G. A. Somorjai, Nature, 258, 580 (1975).
11. D. W. Blakely and G. A. Somorjai, J. Catalysis, to be published 1976.
12. T. A. Clarke, R. Mason and M. Tescari, Surface Sci., 30, 553 (1972).
13. L. L. Kesmodel and G. A. Somorjai, Accts. Chem. Res., to be published 1976.
14. M. A. Chesters and G. A. Somorjai, Ann. Rev. Mat. Sci, 5, 99 (1975).
15. J. C. Buchholz and G. A. Somorjai, Accts. Chem. Res., to be published 1976.

16. L. L. Kesmodel and L. M. Falicov, Solid State Comm., 16, 1201 (1975).

17. Y. W. Tsang and L. M. Falicov, J. Phys. C. Solid State Phys., 9, 51 (1976).

18. Y. W. Tsang and L. M. Falicov, Phys. Rev. B, 12, 2441 (1975).

19. M. A. Chesters and G. A. Somorjai, Surface Sci., 52, 21 (1975).

20. D. I. Hagen, B. E. Nieuwenhuys, G. Rovida and G. A. Somorjai, Surface Sci., to be published 1976.

21. B. E. Nieuwenhuys, D. I. Hagen, G. Rovida and G. A. Somorjai, Surface Sci., to be published 1976.

22. G. A. Somorjai, Surface Sci., 34, 156 (1973).

23. F. J. Szalkowski and G. A. Somorjai, J. Chem. Phys., 54, 389 (1971).

24. J. L. Gland and G. A. Somorjai, Adv. in Colloid and Interface Sci., 5, 203 (1976).

25. L. L. Kesmodel, P. C. Stair, R. C. Baetzold and G. A. Somorjai, Phys. Rev. Lett., to be published 1976.

26. S. H. Overbury, P. A. Bertrand and G. A. Somorjai, Chem. Revs., 75, 547 (1975).

27. S. H. Overbury and G. A. Somorjai, Disc. Meetings of the Faraday Soc., 60, 279 (1975).

28. S. H. Overbury and G. A. Somorjai, Surface Sci., 55, 209 (1976).

29. S. L. Bernasek and G. A. Somorjai, J. Chem. Phys., 60, 4552 (1974).

30. S. L. Bernasek and G. A. Somorjai, J. Chem. Phys., 62, 3149 (1975).

31. B. J. Wood and H. Wise, Surface Sci., 52, 151 (1975).

32. J. Ferrante, Acta Metallurgica, 19, 743 (1971).

33. J. M. McDavid and S. C. Fain, Surface Sci., 52, 161 (1975).

34. S. Thomas, Appl. Phys. Lett., 24, 1 (1974).

35. J. J. Burton, C. R. Helms and R. S. Polizzotti, J. Vac. Sci. Technol., 13, 204 (1976).

36. C. R. Helms and K. Y. Yu, J. Vac. Sci. Technol., 12, 276 (1975).

37. C. R. Helms, J. Catalysis, 36, 114 (1975).

38. S. Berglund and G. A. Somorjai, J. Chem. Phys., 59, 5537 (1973).

39. C. T. H. Stoddart, R. L. Moss and D. Pope, Surface Sci., 53, 241 (1975).

40. C. Leygraf, G. Hultquist, S. Ekelund and J. C. Eriksson, Surface Sci., 46, 157 (1974).

41. R. Bouwman, L. H. Toneman, and A. A. Holscher, Surface Sci., 35, 8 (1973).

42. J. N. Smith and R. L. Palmer, J. Chem. Phys., 56, 13 (1972).

43. H. P. Bonzel and R. Ku, Surface Sci., 33, 91 (1975).

44. J. N. Smith, R. L. Palmer and D. A. Vroom, J. Vac. Sci. and Technol., 10, 5027 (1968).

45. M. Balooch and D. R. Olander, J. Chem. Phys., 63, 4772 (1975).

46. R. A. Krakowski and D. R. Olander, J. Chem. Phys., 49, 5027 (1968).

47. R. J. Madix, Reactive Scattering from Solid Surfaces in Physical Chemistry of Fast Reactions, Vol. 2, D. O. Hayward (Ed.), Plenum, 1976.

48. J. D. McKinley, J. Chem. Phys., 40, 120 (1964).

49. D. R. Olander, R. H. Jones, J. A. Schwartz, W. J. Siekhaus, J. Chem. Phys., 57, 421 (1972).

50. J. B. Anderson and M. Boudart, J. of Catalysis, 3, 216 (1964); R. J. Madix and M. Boudart, J. of Catalysis, 7, 240 (1967).

51. R. J. Madix and A. A. Susu, Surface Sci., 20, 377 (1970).

52. R. J. Madix, R. Parks, A. A. Susu and J. A. Schwartz, Surface Sci., 24, 288 (1971).

53. R. J. Madix and A. A. Susu, J. Vac. Sci. and Technol., 9, 915 (1972).

Table I

Adsorbate-Substrate Bond Lengths Determined by LEED[15]

Substrate	Adsorbate	Bond Length (experimental)	Bond Length (predicted)
Ni(001)	O	1.97 Å	1.90 Å
	S	2.18 Å	2.28 Å
	Se	2.27 Å	2.41 Å
	Te	2.58 Å	2.61 Å
	Na	3.37 Å	3.10 Å
Ni(110)	O	1.91 Å	1.90 Å
	S	2.17 Å	2.28 Å
Ni(111)	S	2.02 Å	2.28 Å
Ag(001)	Se	2.80 Å	2.61 Å
Ag(111)	I	2.75 Å	2.77 Å
Al (100)	Na	3.52 Å	3.32 Å
Mo(001)	N	2.02 Å	2.03 Å
W(110)	O	2.08 Å	2.05 Å

Table II

Surface Enrichment of Binary Metal Alloys

System	Object
Ag-Au[28]	Ag
Ag-Pd[31]	Ag
Al-Cu[32]	Al
Au-Cu[33]	Au
Au-In[34]	In
Au-Ni[35]	Au
Cu-Ni[36,37]	Cu
In-Pb[38]	Pb
Ni-Pd[39]	Pd
Fe-Cr[40]	Cr
Pt-Sn[41]	Sn

Table III

Pre-exponential Factors, Activation Energies and Reaction Probabilities for Several Surface Reactions Studied by Molecular Beam Scattering

Reaction	A*	E_a(kcal/mole)	Reaction Probability	Reference
$H+D_2 \xrightarrow{Pt} HD$ (<600 K)	2×10^5 (sec^{-1})	4.5	$\sim10^{-1}$	30
$H+D_2 \xrightarrow{Pt} HD$ (>600 K)	1×10^2 (sec^{-1})	0.6	$\sim10^{-1}$	30
$D+O_2 \xrightarrow{Pt} D_2O$ (700 K)	-	12	-	42
$CO+O \xrightarrow{Pt} CO_2$ (700 K)	-	20	$\sim10^{-3}$	43
$C_2H_4+O_2 \xrightarrow{Ag} CO_2$ (800 K)	-	8	$<10^{-2}$	44
$2H \xrightarrow{graphite} H_2$ (800-1000 K)	1.06×10^{-2} cm^2/atom sec	15.9	10^{-3}-10^{-2}	45
$H_2 \xrightarrow{Ta} 2H$ (1100-2600 K)	-	75	4×10^{-1}	46
$HCOOH \xrightarrow[decomp]{Ni} CO_2$ (<455 K)	10^{12} (sec^{-1})	20.7	-	47
$HCOOH \xrightarrow[decomp]{Ni} CO_2$ (>455 K)	5.8×10^{13} (sec^{-1})	2.5	~0.9	47
$C+O_2 \longrightarrow CO$ (1000-2000 K)	2.5×10^7 (sec^{-1})	30	10^{-3}-10^{-2}	49
$C+O_2 \longrightarrow CO$ (1000-2000 K)	3×10^{12} (sec^{-1})	50	10^{-3}-10^{-2}	49
$C+4H \longrightarrow CH_4$ (500-800 K)	1.27×10^{-18} cm^4/atom sec	3.3	10^{-3}-10^{-2}	45
$2C+2H \longrightarrow C_2H_2$ (>1000 K)	1.59 cm^2/atom sec	32.5	10^{-3}-10^{-2}	45
$Ge+O_2 \longrightarrow GeO$ (750-1100 K)	10^{16} (sec^{-1})	55	2×10^{-2}	50

Table II (continued)

Reaction	A*	E_a (kcal/mole)	Reaction Probability	Reference
$Ge+O \rightarrow GeO$ (750-1100 K)	10^{16} (sec^{-1})	55	3×10^{-1}	51
$Ge+O_3 \rightarrow GeO$ (750-1100 K)	10^{16} (sec^{-1})	55	5×10^{-1}	52
$Ge+Cl_2 \rightarrow GeCl_2$ (750-1100 K)	10^{7} (sec^{-1})	25	3×10^{-1}	47
$Ge+Br_2 \rightarrow GeBr_2$ (750-1100 K)	10^{7} (sec^{-1})	20	3×10^{-1}	53
$\searrow GeBr_4$				
$Si+Cl_2 \rightarrow SiCl_2$ (1100-1500 K)	10^{8} (sec^{-1})	40	3×10^{-1}	47
$Ni+Cl_2 \rightarrow NiCl$ (900-1400 K)	10^{7} (sec^{-1})	30	8×10^{-1}	48

* For bimolecular reactions, the pre-exponential factor also includes the surface concentration of one of the reactants that is held constant during the experiments.

Figure Captions

Fig. 1 Model of heterogeneous solid surface depicting different surface sites. These sites are distinguishable by their number of nearest neighbors.

Fig. 2 Crystallographic model of a small particle.

Fig. 3 a) Scheme of the low-energy electron diffraction (LEED) experiment. b) Low-energy electron diffraction patterns and schematic representations of the surface configurations of platinum single crystal surfaces: a) Pt(111) containing less than 10^{12} defect/cm^2; b) Pt(557) surface containing 2.5×10^{14} atom/cm^2 with an average spacing between steps of 6 atoms and c) Pt(679) surface containing 2.3×10^{14} step atom/cm^2 and 7×10^{14} kink atoms/cm^2 with an average spacing between steps of 7 atoms and between kinks of 3 atoms.

Fig. 4 a) Diffraction pattern from the Pt(100)-(5x1) structure. b) Schematic representation of the (100) surface with hexagonal overlayer. c) Diffraction pattern from the Pt(100)-(1x1) structure. d) Schematic representation of the (100) surface.

Fig. 5a,b The cutting angles necessary to obtain stepped and kinked surfaces whose schematic diagrams are shown.

Fig. 6 A stereographic triangle of a platinum crystal depicting the various high Miller index surfaces of platinum that were studied.

Fig. 7 Trial geometries of C_2H_2 on the Pt(111) surface. Divisions a, b and c refer to coordination to 1, 2 or 3 neighboring platinum atoms. The labels 1 and 2 distinguish 90° rotated molecules.

Fig. 8 Auger spectra of Au-Ag alloys and of pure Au and Ag.

Fig. 9 Scheme of the molecular beam-surface scattering experiment.

Fig. 10 a) Scattering distribution of H_2 from a clean surface; b) Scattering distribution of H_2 from a CO covered surface.

Fig. 11 a) Angular distribution of H_2 and D_2 scattered from Pt(111) single crystal (HD signal is undetectable). b) Angular distribution of H_2-D_2 and HD scattered from a stepped platinum single crystal. Schematic diagrams of the surfaces are shown above the figures.

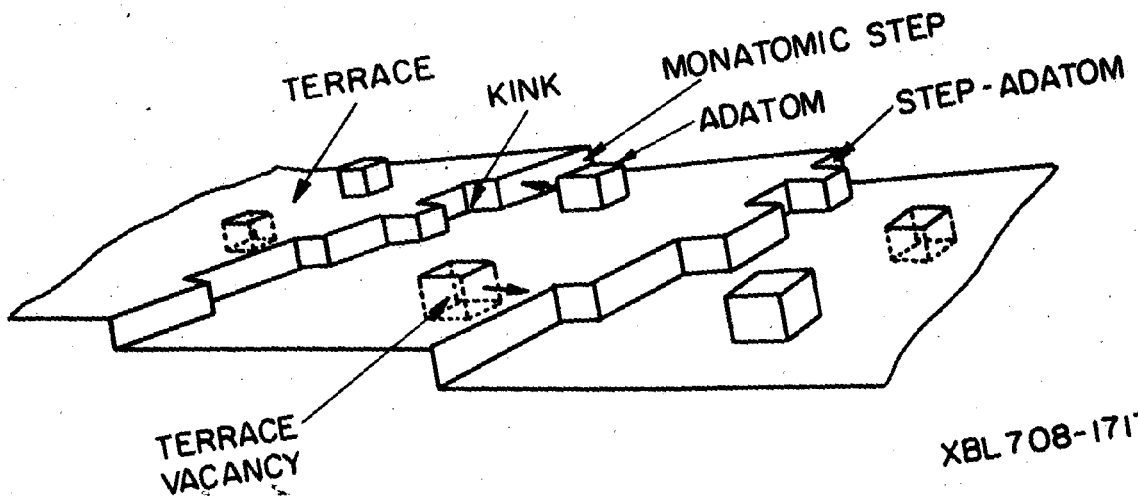

Fig. 1

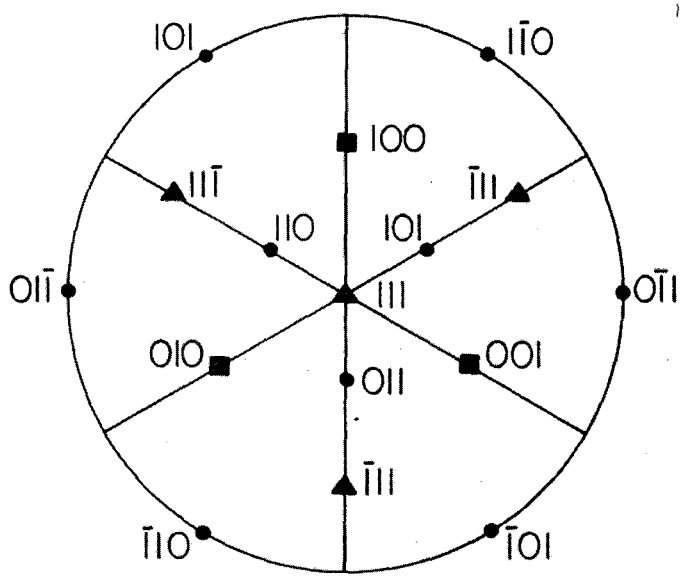

Standard Cubic (111) Projection

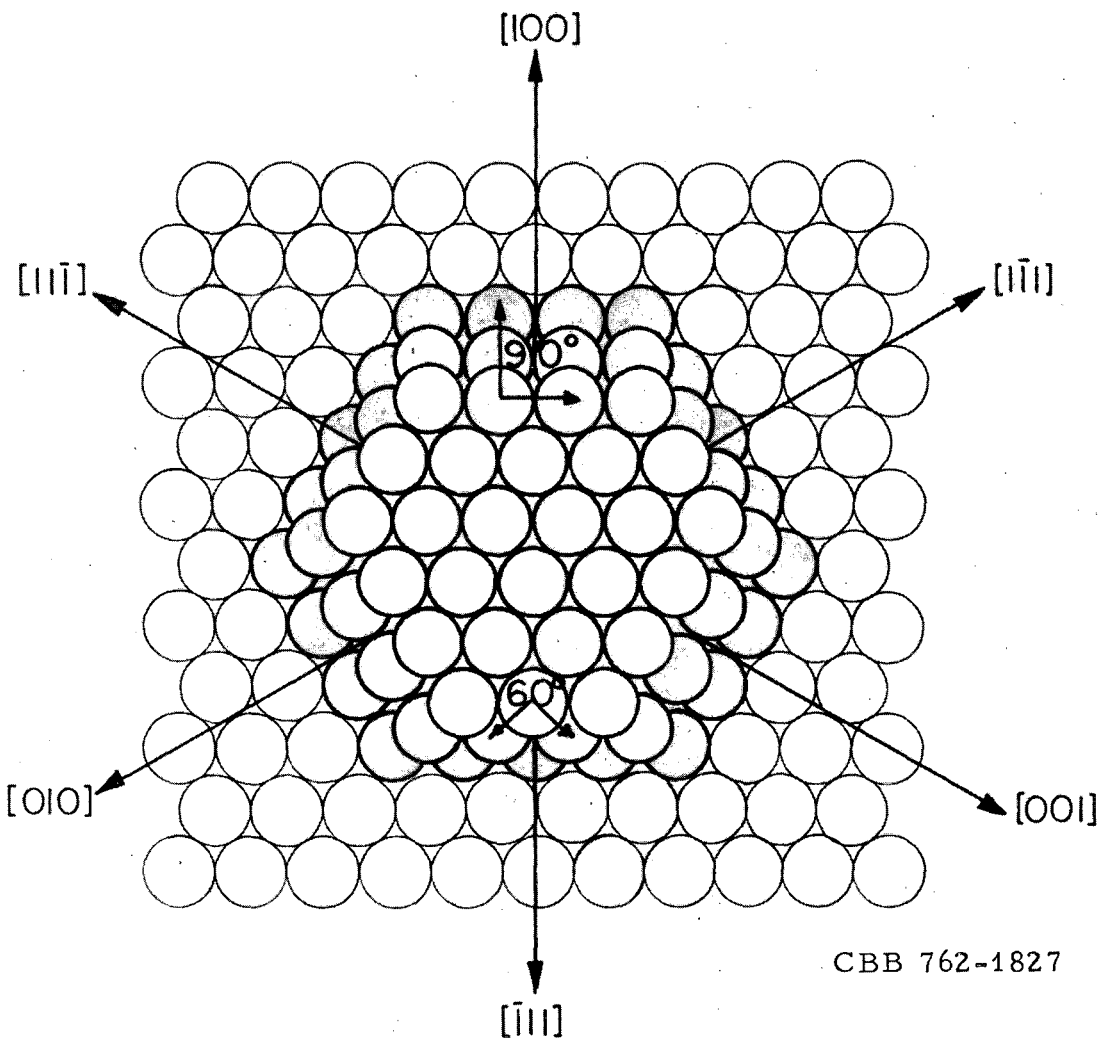

Fig. 2

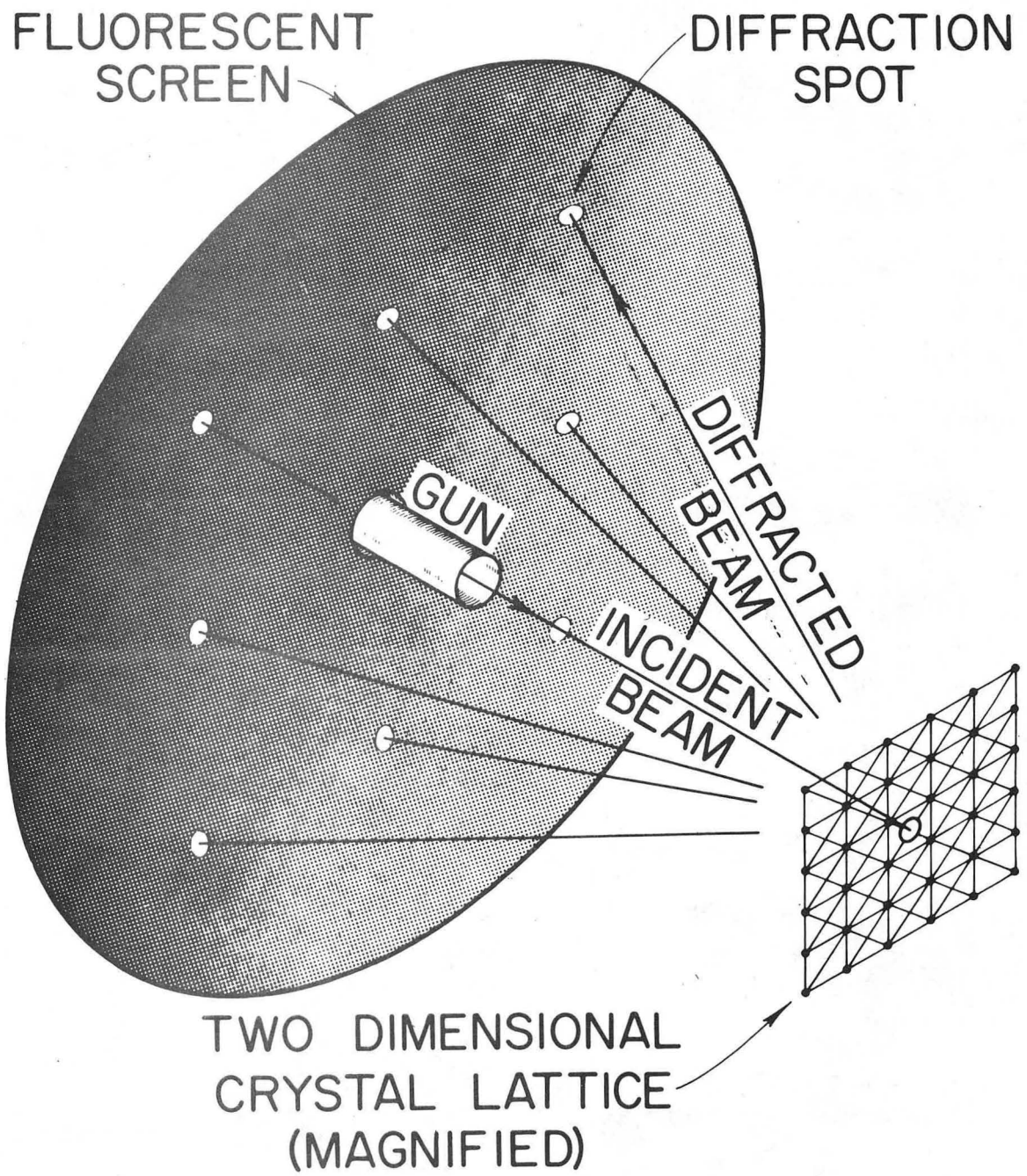

XBB 708-3583

Fig. 3

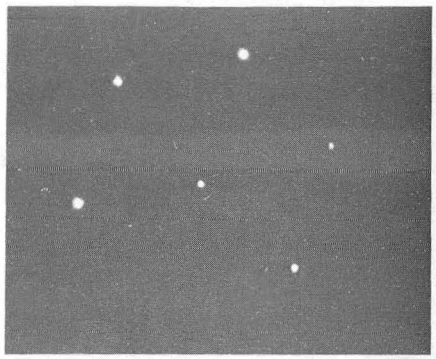

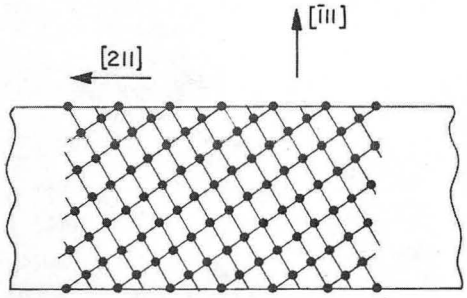

a) Pt - ($\bar{1}11$)

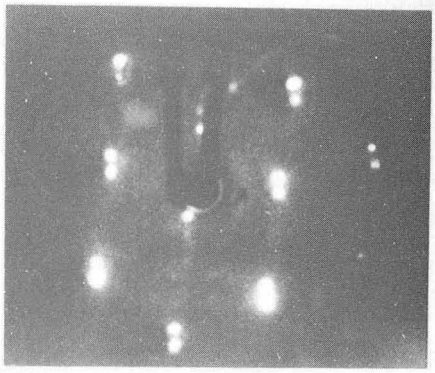

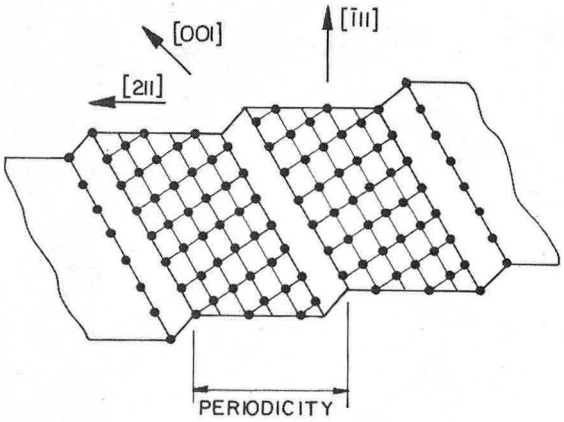

b) Pt - ($\bar{5}57$)

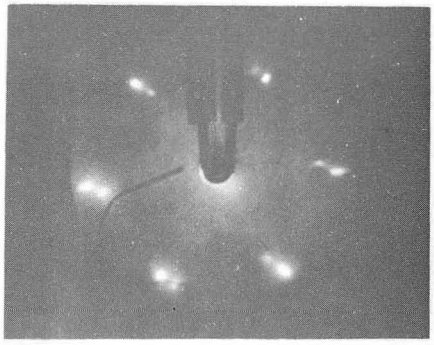

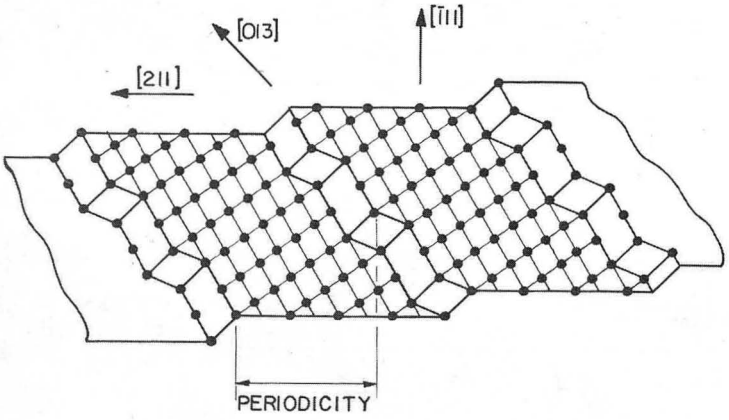

c) Pt - ($\bar{6}79$)

XBB 758-5903

Fig. 4

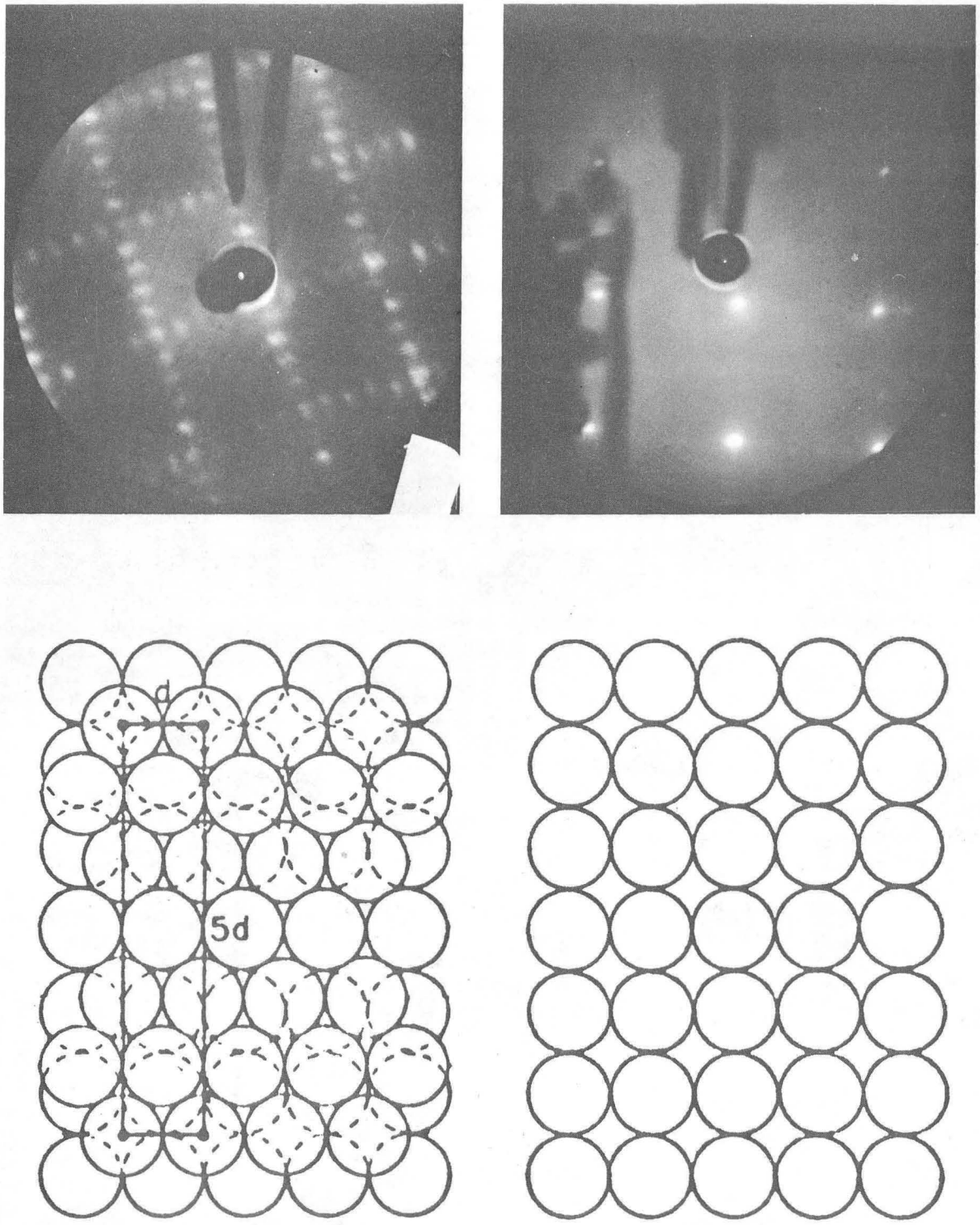

XBB 711-5356

Fig. 5

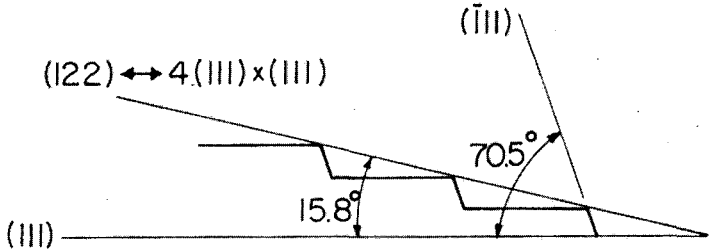

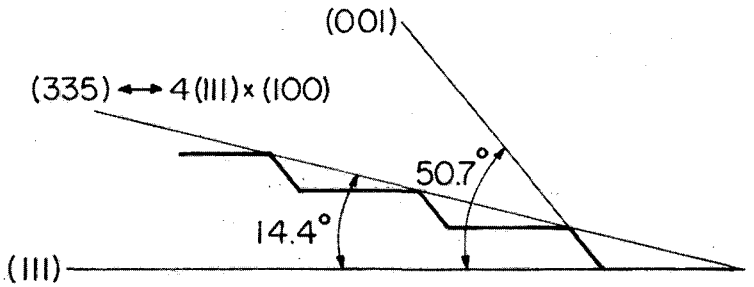

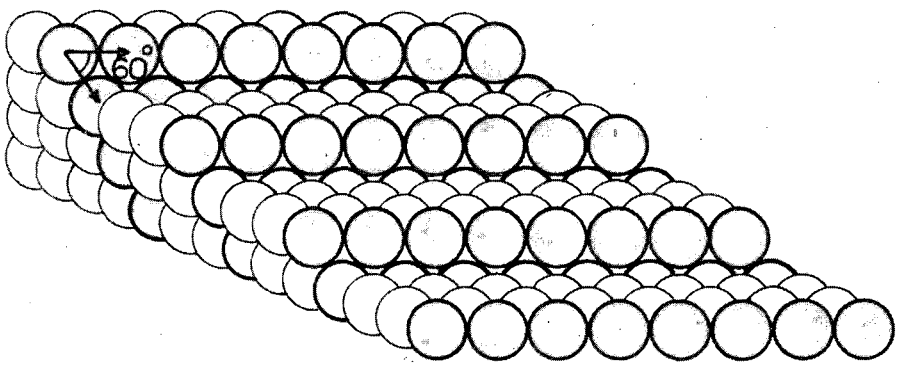

Face-Centered Cubic (122) ↔ 4(111) x (111)

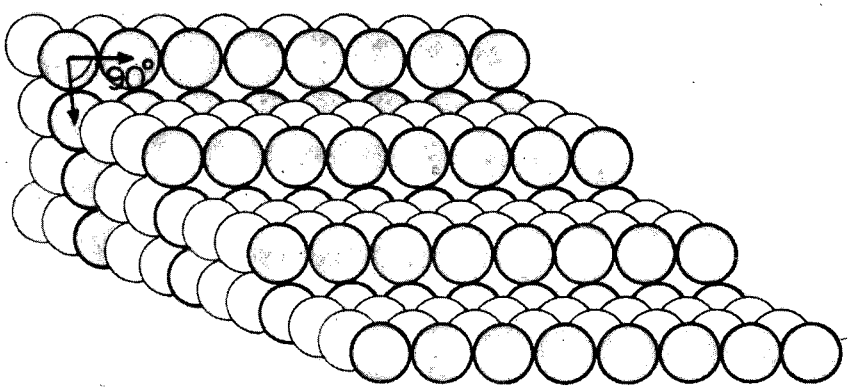

Face-centered Cubic (335) ↔ 4(111) x (100)

CBB 762-1819

Fig. 6

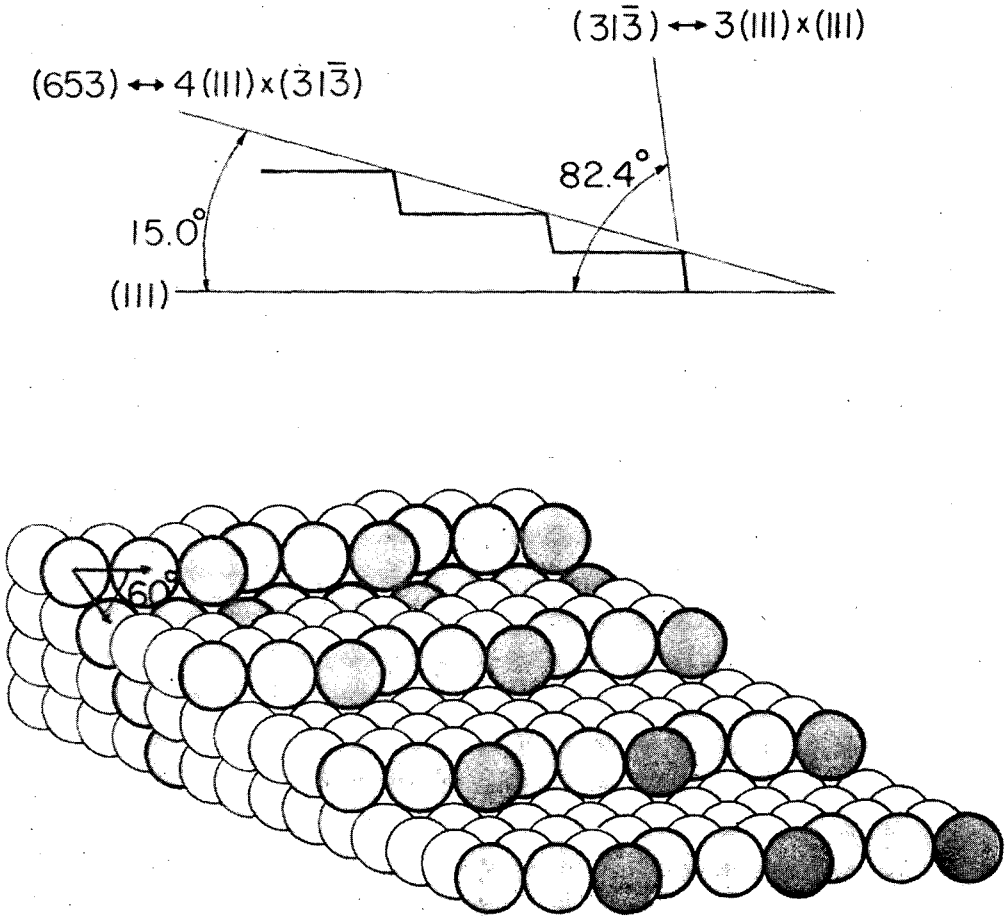

Face-Centered Cubic (653) ↔ 4(111)x(31$\bar{3}$)

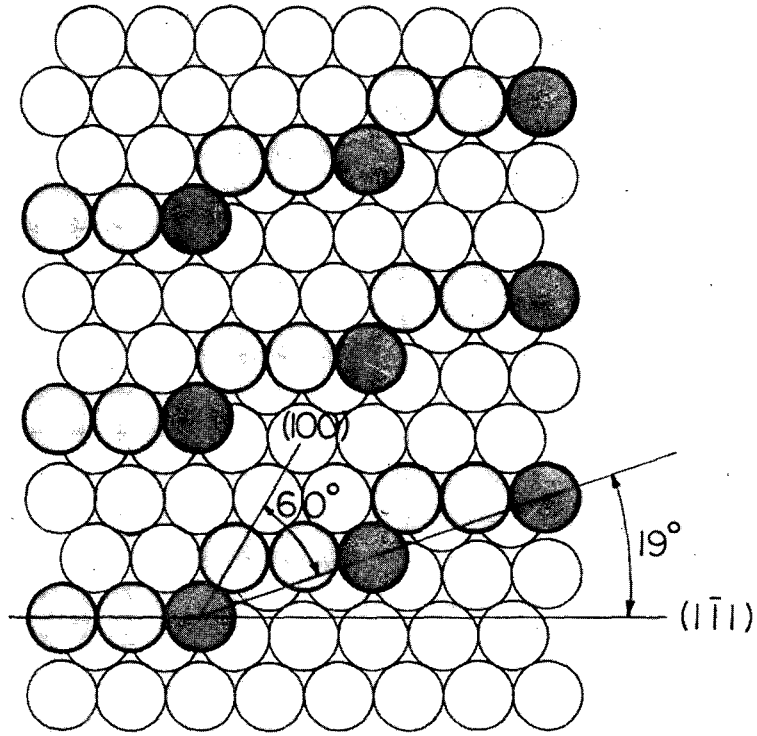

CBB 762-1829

Fig. 7

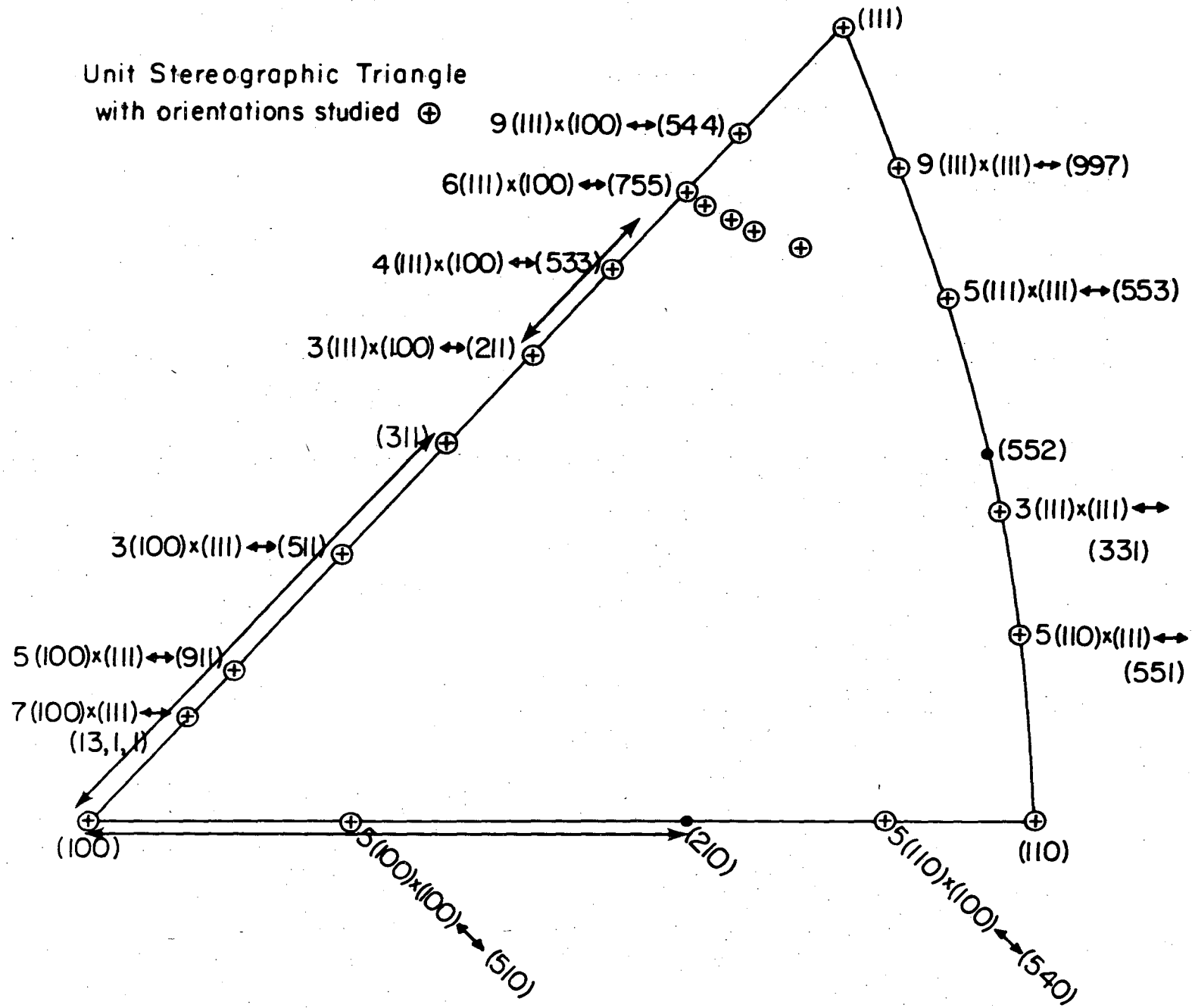

CBB 756-4244

Fig. 8

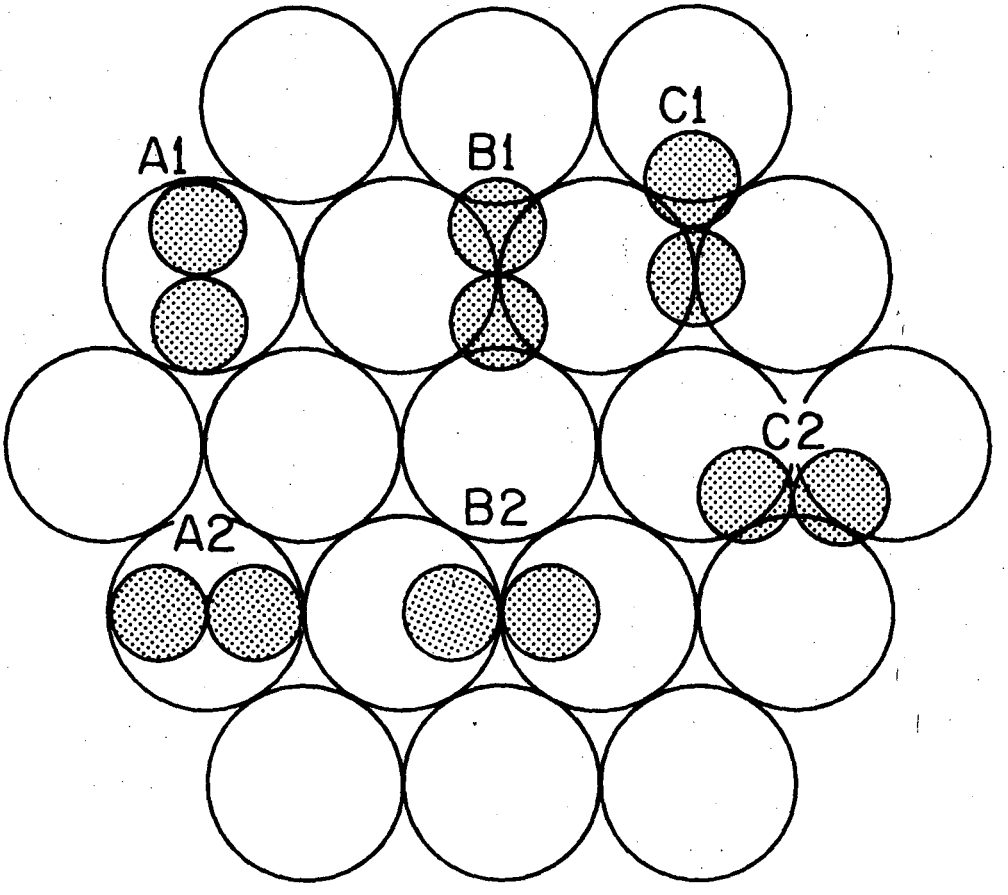

Fig. 9

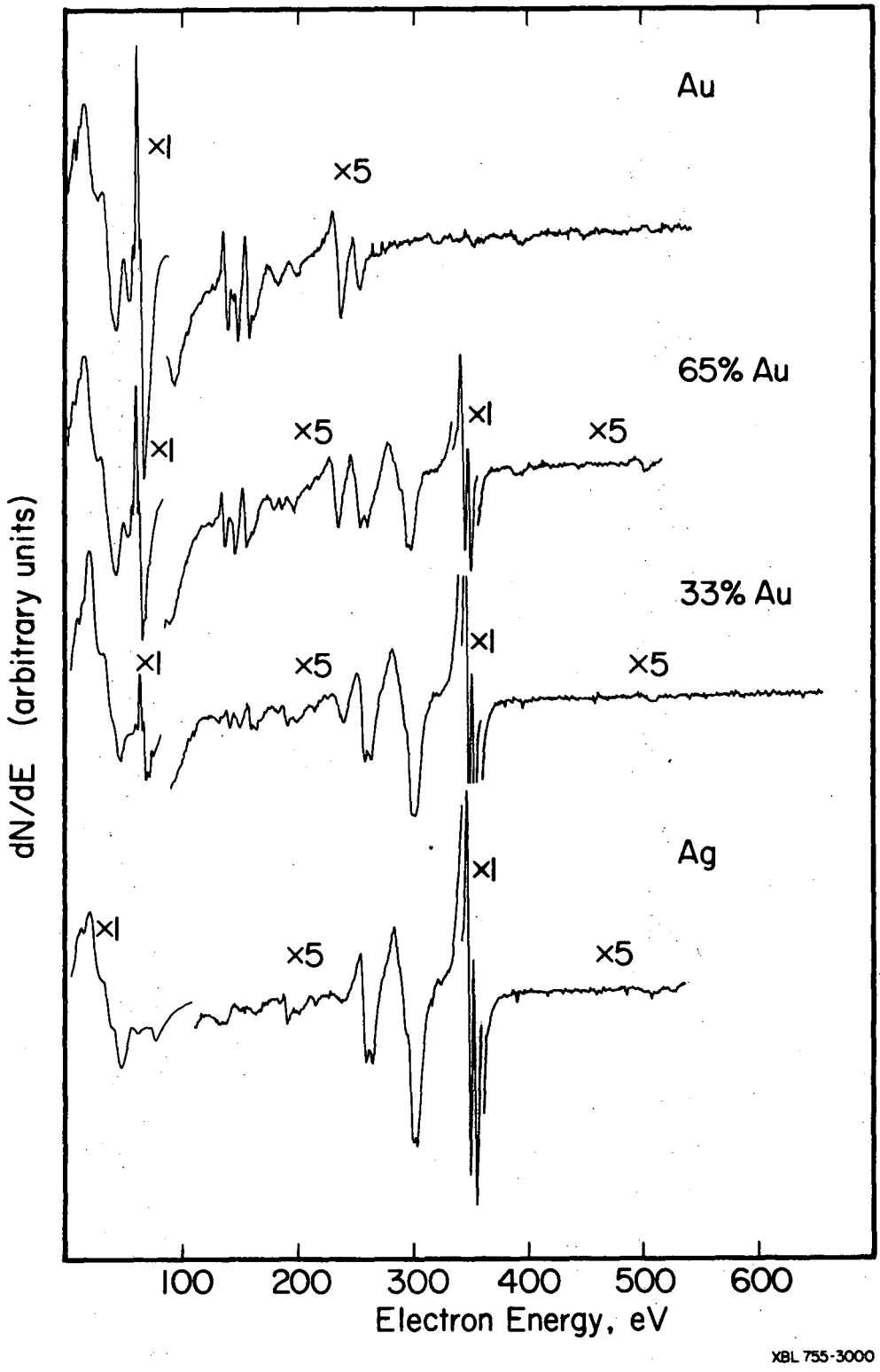
Au
×1
×5
65% Au
×1
×5
×1
×5
33% Au
×1
×5
×1
×5
Ag
×1
×5
×1
×5
dN/dE (arbitrary units)
100
200
300
400
500
600
Electron Energy, eV
XBL 755-3000

Fig. 10

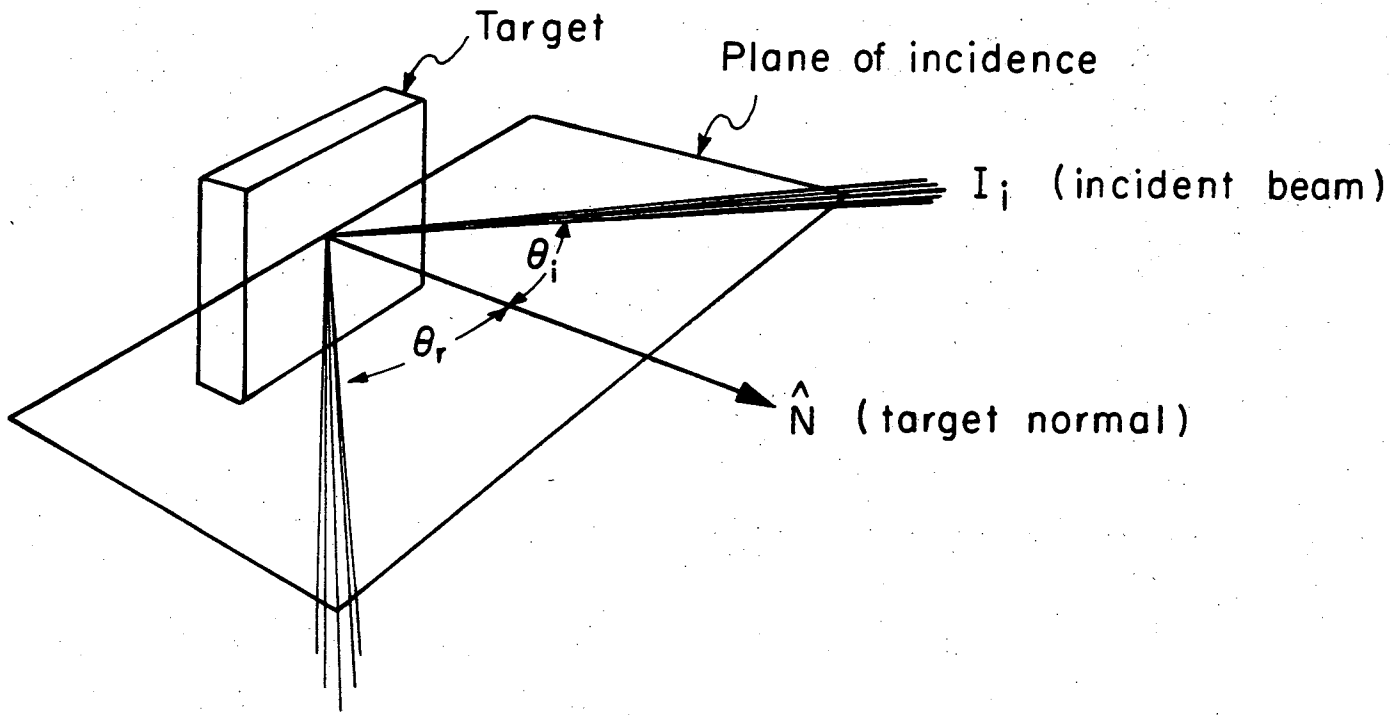

XBL 708-1973

Fig. 11

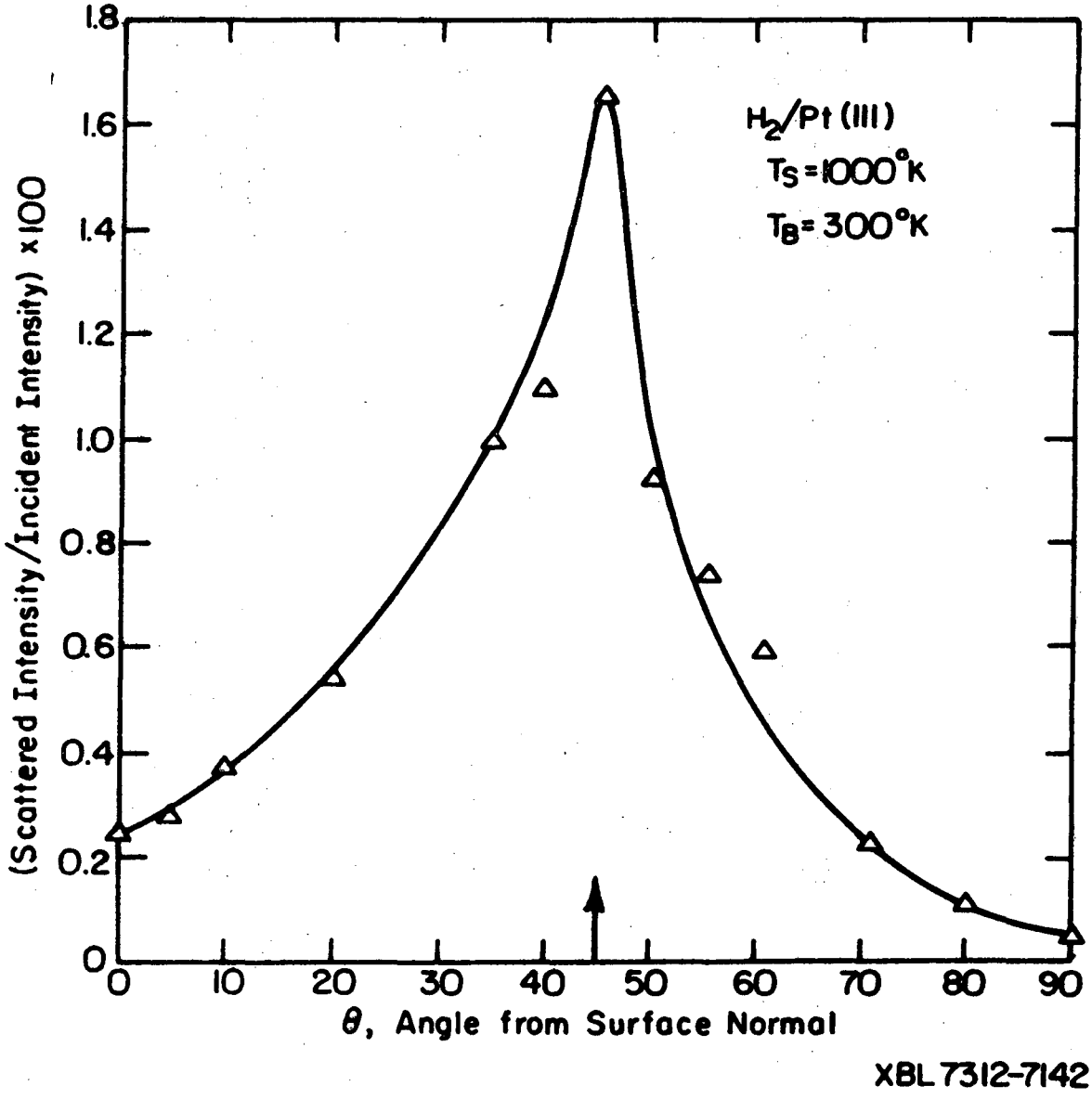
H2/Pt (111)
TS = 1000°K
TB = 300°K
(Scattered Intensity/Incident Intensity) x100
θ, Angle from Surface Normal
0
0.2
0.4
0.6
0.8
1.0
1.2
1.4
1.6
1.8
0
10
20
30
40
50
60
70
80
90
XBL 7312-7142

Fig. 12

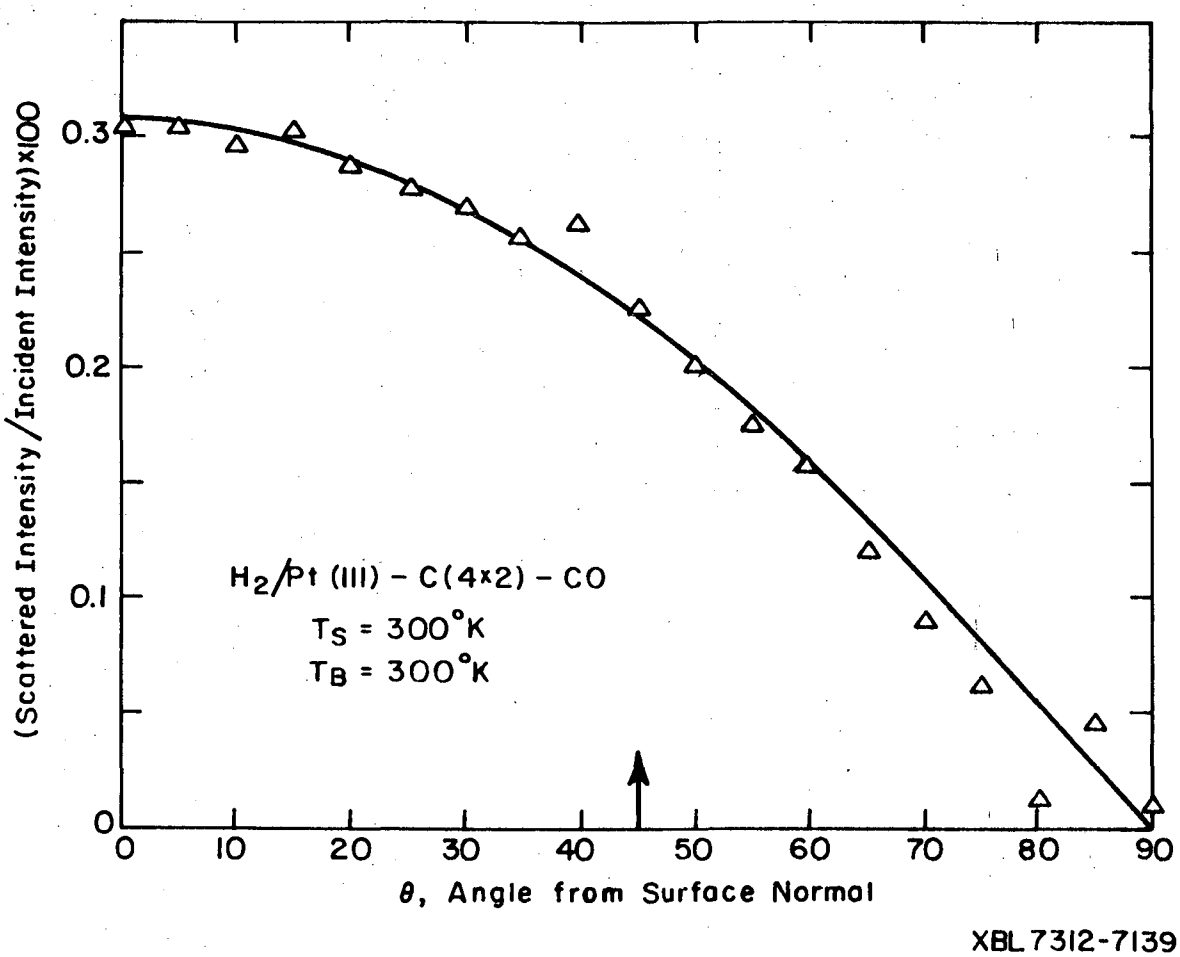

Fig. 13

This report was done with support from the United States Energy Research and Development Administration. Any conclusions or opinions expressed in this report represent solely those of the author(s) and not necessarily those of The Regents of the University of California, the Lawrence Berkeley Laboratory or the United States Energy Research and Development Administration.

TECHNICAL INFORMATION DIVISION
LAWRENCE BERKELEY LABORATORY
UNIVERSITY OF CALIFORNIA
BERKELEY, CALIFORNIA 94720